

## Article

# Effect of Grinding Media Size on Ferronickel Slag Ball Milling Efficiency and Energy Requirements Using Kinetics and Attainable Region Approaches

Evangelos Petrakis \*  and Konstantinos Komnitsas \* 

School of Mineral Resources Engineering, Technical University of Crete, 73100 Chania, Greece

\* Correspondence: vpetraki@mred.tuc.gr (E.P.); komni@mred.tuc.gr (K.K.); Tel.: +30-28210-37608 (E.P.); +30-28210-37686 (K.K.)

**Abstract:** The aim of this study is to evaluate the effect that the size of grinding media exerts on ferronickel slag milling efficiency and energy savings. A series of tests were performed in a laboratory ball mill using (i) three loads of single size media, i.e., 40, 25.4, and 12.7 mm and (ii) a mixed load of balls with varying sizes. In order to simulate the industrial ball milling operation, the feed to the mill consisted of slag with natural size distribution less than 850  $\mu\text{m}$ . Grinding kinetic modeling and the attainable region (AR) approach were used as tools to evaluate the data obtained during the ball milling of slag. Particular importance was given to the determination of the specific surface area of the grinding products, the identification of the grinding limit, and the maximum specific surface area which could be achieved when different grinding media sizes were used. The results showed that, in general, the breakage rates of particles obey non-first-order kinetics and coarse particles are ground more efficiently than fines. The AR approach proved that there is an optimal grinding time (or specific energy input) dependent on the ball size used for which the volume fraction of the desired size class is maximized. The use of either 25.4 mm balls or a mixed load of balls with varying sizes results in 31 and 24% decrease in energy requirements, compared to the use of balls with small size (12.7 mm).

**Keywords:** ball size effect; slag; grinding; kinetic modeling; specific surface area; energy requirements; specific energy; attainable region approach



**Citation:** Petrakis, E.; Komnitsas, K. Effect of Grinding Media Size on Ferronickel Slag Ball Milling Efficiency and Energy Requirements Using Kinetics and Attainable Region Approaches. *Minerals* **2022**, *12*, 184. <https://doi.org/10.3390/min12020184>

Academic Editors: Thomas Mütze and Chiharu Tokoro

Received: 27 December 2021

Accepted: 28 January 2022

Published: 30 January 2022

**Publisher's Note:** MDPI stays neutral with regard to jurisdictional claims in published maps and institutional affiliations.



**Copyright:** © 2022 by the authors. Licensee MDPI, Basel, Switzerland. This article is an open access article distributed under the terms and conditions of the Creative Commons Attribution (CC BY) license (<https://creativecommons.org/licenses/by/4.0/>).

## 1. Introduction

Slags generated from the non-ferrous, ferrous and steel industries, as well as residues produced from various hydrometallurgical operations, are becoming a subject of great environmental and ecological debate [1]. At present, large volumes of slags containing toxic elements, such as chromium, lead, and cadmium, are disposed of on land or underwater and cause serious contamination of water resources and soil [2]. However, slags have found a wide range of applications in the construction, cement, and fertilizers industries, and can be considered as secondary sources for base metals, especially iron and copper [3]. Previous studies indicate that certain metals can be effectively extracted from slags using hydro- and pyro-metallurgical processes, as well as several beneficiation techniques [4–7]. In recent years, the alkali activation of various slags for the production of materials or binders that can be used in construction applications is extensively investigated [8,9]. As a result, the increase of the utilization rate of slags and the development of sustainable management schemes for environmental protection are of great importance for both the industry and the society [10–12].

Prior to carrying out any further processing of slags, comminution or size reduction, which involves two operations, crushing and grinding, is required. Comminution, especially grinding, is characterized by low efficiency, high CO<sub>2</sub> emissions, and increased process cost. More specifically, it has been proven that the total amount of energy used by

the mining and minerals industry is 4–7% of the global energy output [13]. For a typical grinding circuit, the average energy consumption can be as high as 6700 kWh/kt, and represents almost 50% of the total energy consumption in the mining industry [14,15]. This high energy consumption and the associated CO<sub>2</sub> emissions from comminution circuits can be reduced if the grinding behavior of the feed is carefully investigated as a function of the operating parameters of the crusher/mill. In addition, apart from the energy savings and the associated economic benefits, the valorization of metallurgical slags will result in considerable savings of natural resources and the reduction of the environmental footprint of various industrial sectors, including metallurgy and construction [16,17].

Grinding of ores has been extensively studied for over 150 years. During this period, empirical energy-size reduction relationships were first used, while more recently equations that take into account the particle size distribution of the feed and the products were developed [18]. Over the past decades, several studies have been carried out for the development of phenomenological grinding kinetic models. The so-called population balance model (PBM) can be used for the design, optimization, and control of grinding circuits due to its ability to take into account the breakage mechanism [19–21]. The PBM, also referred to as the linear time-invariant (LTINV) model, which considers that the breakage rate remains constant during grinding has been adopted by many researchers [22–25], while in other studies a deviation from the linear kinetic approach has been experimentally observed [26–28]. Recently, Petrakis and Komnitsas [15] used the PBM as partial case and developed a non-linear framework for the prediction of the particle size distribution of the grinding products. Nevertheless, the linear kinetic approach has been successfully used for understanding the effect of operating parameters, e.g., ball size, mill speed, media shape, and ball/powder filling, on the grinding efficiency of ball mills [29–35].

Austin et al. [19] developed the batch grinding equation of the PBM in its time continuous size-discretized form, as shown in Equation (1),

$$\frac{dR_i(t)}{dt} = -S_i R_i(t) + \sum_{j=1}^{i-1} S_j b_{ij} R_j(t), \quad i \geq j \geq 1 \quad (1)$$

where  $R_i(t)$  is the mass/volume fraction for size class  $i$  at grinding time  $t$ ,  $S_i$  is the breakage rate function of size class  $i$ , and  $b_{ij}$  is the breakage distribution function representing the mass/volume fraction of the broken products with size  $j$  that appears in the size class  $i$ .

Considering that the breakage rate  $S_i$  is constant during grinding and breakage follows a first-order law, Equation (1), for  $i = 1$ , can be expressed as,

$$\frac{dR_1(t)}{dt} = -S_1 R_1(t) \quad (2)$$

or

$$R_1(t) = R_1(0) \exp(-S_1 t) \quad (3)$$

where  $R_1(0)$  is the mass/volume fraction for size class 1 (coarse fraction) at time 0,  $R_1(t)$  is the fraction for size class 1 at grinding time  $t$ , and  $S_1$  is the breakage rate of size class 1.

Furthermore, with respect to size class 2, Equations (4) and (5) can be obtained (for  $i = 2$  in Equation (1)),

$$\frac{dR_2(t)}{dt} = -S_2 R_2(t) + b_{21} S_1 R_1(t) \quad (4)$$

or

$$R_2(t) = R_2(0) \exp(-S_2 t) + \frac{b_{21} S_1 R_1(0)}{S_2 - S_1} [\exp(-S_1 t) - \exp(-S_2 t)] \quad (5)$$

When the non-first order grinding behavior is considered, Alyavdin proposed the following formula (Equation (6)) in ball milling processes [36],

$$R_i(t) = R_i(0) \exp(-Kt^M) \quad (6)$$

where  $K$  is the grinding rate constant, and  $M$  is a constant depending on the feed properties and grinding conditions. If  $M \neq 1$  grinding follows non-first-order kinetics.

In recent years, a model-free approach called the attainable region (AR) method has been introduced, in order to better design comminution circuits and also optimize the parameters affecting the grinding process [37]. The AR method was first applied for the optimization of chemical processes [38], while later it was introduced into the comminution circuits [39]. Its concept is based on the optimization of the grinding process by maximizing the concentration of the desired (target) product size for the least possible energy consumption [40]. It is known that the primary target of comminution is the production of a desired product size for separation operations and the liberation of the valuable minerals present in ores [41]. Any separation operation will only be effective if an appropriate size is used, while if the feed is extensively ground the produced ultra-fines, apart from the grinding cost increment, will reduce the efficiency of the separation. For example, in the flotation process, it has been found that extremely fine particles (e.g.,  $<20 \mu\text{m}$ ) have lower collision efficiency with bubbles and this results in losses of valuable minerals [42]. In addition, regarding the leaching process, although finely ground raw material with large surface area is usually required for efficient extraction of valuable metals, recent research studies indicate that for certain ores there is a specific size fraction for which a maximum leaching rate is observed [43,44]. In this context, the AR method may be used to determine the optimal parameters of the grinding process, i.e., residence time, media/feed size, and media filling ratio, which maximize the desired size range of grinding products [23,44–48].

The objective of this study is to improve the ball milling efficiency of ferronickel slag and determine the optimal grinding media size for which coarse particles are effectively reduced or the fraction of the desired size class is maximized, while at the same time energy consumption is reduced. In order to achieve this, grinding kinetics modeling and the AR approach were used to evaluate data obtained from the milling of slag. The Brunauer–Emmett–Teller (BET) technique was also used to determine the grinding limit and the maximum specific surface area that can be obtained for different operating conditions. The optimization of the grinding of slag, will not only result in reduced operating cost, but also in the improvement of sustainability of the metallurgical, construction, and other industries. In addition, by considering the principles of zero waste and circular economy, the valorization of industrial wastes and by-products, as the slag used in this study, will result in the conservation of natural resources and the reduction of their impact on the environment.

## 2. Materials and Methods

In this study ferronickel slag produced after pyrometallurgical treatment of lateritic ores the period 1900–1982 in Szklary, Lower Silesia, Poland, was used [49]. The sample was collected from a slag disposal site and its chemical composition, as obtained by X-ray fluorescence in the form of oxides is shown in Table 1. The X-ray diffraction (XRD) analysis revealed that the main mineralogical phases present were quartz ( $\text{SiO}_2$ ), hedenbergite ( $\text{Ca}(\text{Fe},\text{Mg})(\text{SiO}_3)_2$ ), fayalite ( $\text{Fe}_2\text{SiO}_4$ ), diopside ( $\text{CaMgSi}_2\text{O}_6$ ), and magnetite ( $\text{Fe}_3\text{O}_4$ ), while hatrurite ( $\text{Ca}_3\text{SiO}_5$ ) was present as a minor phase. More data about the characteristics of this slag can be found in previous recent studies [11,50].

**Table 1.** Chemical composition of slag.

$\text{Fe}_2\text{O}_3$	$\text{SiO}_2$	$\text{CaO}$	$\text{Al}_2\text{O}_3$	$\text{Cr}_2\text{O}_3$	$\text{MgO}$	$\text{NiO}$	$\text{K}_2\text{O}$	$\text{TiO}_2$	$\text{MnO}$	Total
40.62	30.18	13.00	7.60	1.98	1.80	0.95	0.89	0.69	0.28	97.99

About 200 kg of slag, with a particle size of less than 100 mm, were received. A sub-sample of 20 kg was crushed to less than 0.850 mm using a Fritsch type jaw crusher (Fritsch pulverisette 1, Fritsch GmbH, Idar-Oberstein, Germany) for primary and a cone crusher (Version, Sepor, Wilmington, NC, USA) for secondary crushing. Representative samples of the crushing products were used as feed in the mill for the grinding tests.

Four series of grinding tests were conducted using a laboratory batch scale ball mill (Version, Sepor, Los Angeles, CA, USA) that operated at 66 rpm (1.1 Hz) corresponding to 70% of its critical speed, under dry conditions, as seen in Table 2. The grinding media consisted of balls with various sizes and density  $7.85 \text{ g/cm}^3$ , corresponding to ball filling volume  $J = 20\%$ , while the material filling volume  $f_c$  was 4%. Consequently, the interstitial void space of the balls  $U$  that is filled with slag was kept constant at 50%, as shown in Equation (7).

$$U = \frac{f_c}{0.4 \cdot J} \quad (7)$$

**Table 2.** Mill specification data and test series conditions.

Item	Description	1st Series	2nd Series	3rd Series	4th Series
Steel Balls	Diameter, $d$ (mm)	40	25.4	12.7	40, 25.4, 12.7
	Number	20	77	603	6, 28, 202
	Weight (g)	5239.2	5128.2	5122.9	1572.7, 1865.7, 1702.4
	Density ( $\text{g/cm}^3$ )	7.85	7.85	7.85	7.85
	Porosity (%)	40	40	40	40
	Ball filling volume, $J$ (%)	20	20	20	20
Item	Description	In All Series			
Ball Mill	Diameter, $D$ (cm)	20.4			
	Length, $L$ (cm)	16.6			
	Volume, $V$ ( $\text{cm}^3$ )	5423			
	Operational speed, $N$ (rpm)	66			
	Critical speed, $N_c$ (rpm)	93.7			
Feed	Bulk density ( $\text{g/cm}^3$ )	1.67			
	Material filling volume, $f_c$ (%)	4			
	Interstitial filling, $U$ (%)	50			

In this test series, three loads with the same mass of single size grinding media (balls), i.e., 40, 25.4, and 12.7 mm diameter were used, while an additional test using a load of balls with varying sizes and equal mass for each size was also run. According to the procedure followed, the feed with size less than 0.850 mm ( $d_{50} = 0.235 \text{ mm}$ ) was ground in the mill for various periods, namely 15, 30, 45, 60, 90, and 120 min, and the particle size distribution (PSD) of the product obtained after each grinding period was determined using a Malvern type S Mastersizer (Version, Malvern Instruments, Malvern, UK) (particle size range between 0.05 and 850  $\mu\text{m}$ ) and laser diffraction (LD) technique.

The power of the mill,  $P$  (kW), based on a large amount of data from laboratory and industrial mills, can be calculated using the following formula [51,52],

$$P = 7.33 \cdot J \cdot N_r \cdot (1 - 0.937 \cdot J) \cdot \rho_b \cdot L \cdot D^{2.3} \cdot \left(1 - \frac{0.1}{2^{9-10 \cdot N_r}}\right) \quad (8)$$

The specific energy  $\varepsilon$  (kJ/kg) input, namely the energy input  $E$  (kJ) per unit mass  $m$  (kg) of the feed, can be expressed in terms of grinding time  $t$  as:

$$\varepsilon = \frac{E}{m} = \frac{P \cdot t}{m} \quad (9)$$

The specific surface area (SSA) of the feed and the grinding products was determined by the LD technique according to Equation (10). It is mentioned that LD uses light-scattering measurements to calculate the volume-based PSD, and assumes a specific geometry for the particles without taking into consideration the particle shape [53,54]. The BET nitrogen adsorp-

tion method (using a Quantachrome Nova 2200 analyzer, Anton Paar QuantaTec Inc., Boynton Beach, FL, USA) was also used in this study for the determination of SSA [55].

$$S_w = \left(\frac{f}{k}\right) \cdot \frac{1}{\rho_p \cdot D[3,2]} \quad (10)$$

where  $S_w$  is the specific surface area,  $\rho_p$  is the particle density,  $D[3,2]$  is the mean surface area (Sauter mean diameter), and  $f, k$  are the surface and volume coefficients (for spheres  $f/k = 6$ ).

### 3. Results and Discussion

#### 3.1. Grinding Kinetics

The grinding behavior of the slag was investigated by identifying the relationship between the remaining (% volume) fraction for six representative particle sizes vs. grinding time, when three loads of grinding media with the same ball size, namely 40 mm, 25.4 mm, 12.7 mm, and an additional load consisting of equal mass of balls from each size were used (Figure 1a–d). The representative selected sizes of the slag were 163.8, 65.51, 26.20, 5.69, 1.68, and 0.49  $\mu\text{m}$ . It is observed from Figure 1a–d that in all cases the remaining fraction of each representative size decreases with increasing grinding time, while the reduction rate depends on the size (diameter) of the grinding media. When Equation (6) was fitted to the experimental data, it was found that grinding of slag exhibits non-first-order behavior and the grinding rate of each particle size is time-dependent. In light of this, very good fitting curves, as indicated by the high values of correlation coefficient  $R^2$  (adj.), ranging from 0.977 to 1.0, were obtained when all types of grinding media were used. In general, as grinding time increases, the reduction rate of coarser particles is higher than that of finer particles, which indicates that coarser particles are ground more efficiently.

The estimated parameters, namely  $K$  and  $M$ , as well as the  $R^2$  (adj.) values obtained after fitting the Alyavdin formula (Equation (6)) to experimental data are presented in Table 3. From this table it is confirmed that, for a given grinding media load, the grinding rate constant ( $K$ ) increases with increasing particle size, and slag grinding follows non-first-order kinetics as indicated by the values of parameter  $M$  which in all cases were not equal to 1 but ranged from 0.682 to 1.077.

Regarding the effect of grinding media size on slag grinding kinetics, Figure 2 presents the grinding rate constant ( $K$ ) values versus the particle size for different ball sizes. It is seen that the use of 25.4 mm balls results in a higher breakage rate, while the respective rate decreases significantly when a mixed load of balls is used; parameter  $K$  ranged from 0.0010 to 0.1546 and 0.005 to 0.0485 when balls with diameter of 25.4 mm or a load consisting of equal mass of balls from each size were used, respectively. It is also revealed that the smallest balls (12.7 mm size) are suitable for efficient grinding of slag ( $K$  ranged from 0.0017 to 0.1333), whereas the use of larger balls (40 mm) results in a much smaller breakage rate ( $K$  ranged from 0.0008 to 0.0614). So far, various attempts have been made to define the optimum grinding media size and improve the efficiency of ball milling [30,56–61]. It has been found that the optimum ball size depends on several factors, including the feed/product size ratio, the mill dimensions, and the breakage parameters. In general, larger balls are needed for the breakage of coarse particles, whereas fine particles are ground more efficiently with the use of smaller balls [62]. However, in industrial mills, the feed which comes from the crushing stage has natural size distribution, and therefore it is common practice to use grinding media consisting of balls with varying sizes for efficient grinding. In the present study, the use of Alyavdin formula indicates that balls with 25.4 mm diameter are suitable for the milling of slag with size smaller than 0.850 mm, whereas the use of balls with varying size results in lower grinding efficiency.

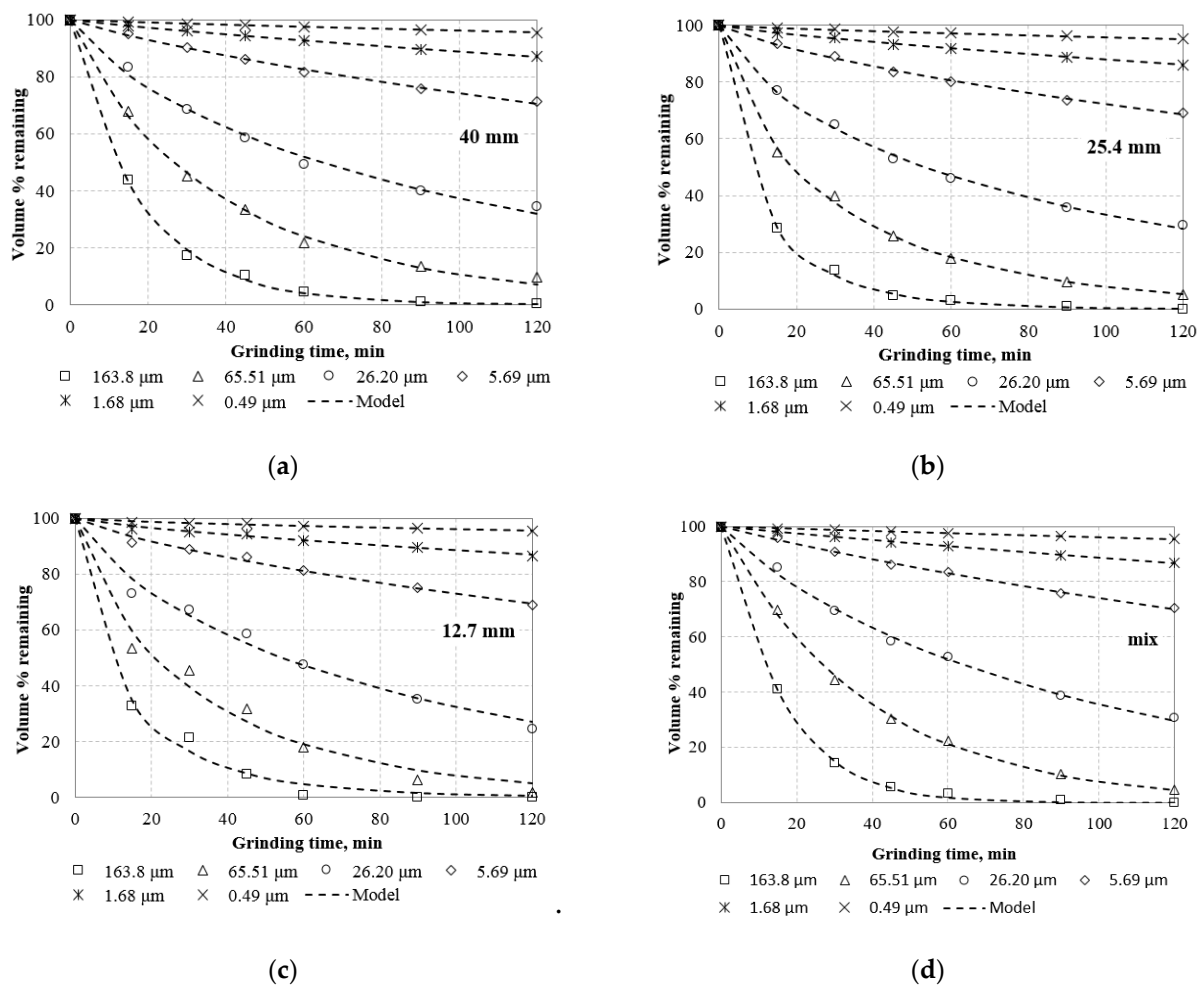


**Figure 1.** Remaining fraction (% volume) for various slag sizes vs. grinding time when equal mass of balls with sizes (a) 40 mm, (b) 25.4 mm, (c) 12.7 mm, and (d) a mixed load of grinding media consisting of equal mass of balls from each of the three sizes were used.

**Table 3.** Parameters of Alyavdin formula (Equation (6)) for six representative slag particle sizes using different ball sizes as grinding media.

Ball Size (mm)	Parameter	163.8 μm	65.51 μm	26.20 μm	5.69 μm	1.68 μm	0.49 μm
40	K	0.0614	0.0370	0.0243	0.0054	0.0020	0.0008
	M	0.966	0.891	0.803	0.872	0.886	0.853
	R <sup>2</sup> (adj.)	0.999	0.997	0.992	0.996	0.999	0.999
25.4	K	0.1546	0.0662	0.0361	0.0079	0.0028	0.0010
	M	0.770	0.792	0.743	0.807	0.835	0.823
	R <sup>2</sup> (adj.)	0.999	0.998	0.998	0.998	0.999	0.998
12.7	K	0.1333	0.0534	0.0277	0.0078	0.0036	0.0017
	M	0.765	0.837	0.806	0.802	0.763	0.682
	R <sup>2</sup> (adj.)	0.999	0.998	0.998	0.998	0.982	0.977
mix *	K	0.0485	0.0255	0.0168	0.0039	0.0015	0.0005
	M	1.077	1.004	0.894	0.943	0.954	0.952
	R <sup>2</sup> (adj.)	1.000	0.999	0.996	0.997	0.998	0.997

\* a mixed load of grinding media consisting of equal mass of balls from each of the three sizes (40, 25.4, and 12.7 mm).

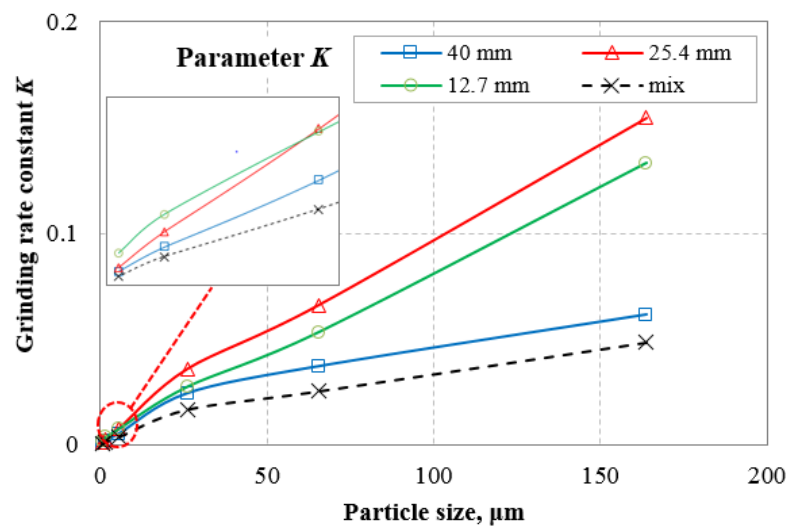


**Figure 2.** Grinding rate constant ( $K$ ) values versus slag particle size for various ball sizes (40 mm, 25.4 mm, 12.7 mm), including a mixed load of grinding media consisting of equal mass of balls from each of the three sizes.

The behavior of slag during grinding was further investigated during the initial grinding stage as well as during prolonged grinding periods. Figure 3a,b present, as an example, the remaining fraction (% volume) of the 163.8  $\mu\text{m}$  particle size of slag vs. grinding time during the first 45 min (initial stage) and after grinding periods up to 120 min (final stage), when balls with varying size were used. It can be seen from Figure 3a that among the grinding media used, the 25.4 mm balls achieve the highest reduction rate, in accordance with the results shown in Figure 2. However, it is apparent that toward the second part of the initial stage (25–45 min), the grinding rate and consequently the grinding efficiency is improved even with the use of balls with varying sizes. In addition, Figure 3b indicates that during the final stages of grinding, it is more efficient to use balls with varying sizes, while the use of the small balls (12.7 mm) results in bigger amount of material that remained in the 163.8  $\mu\text{m}$  particle size. Therefore, grinding of coarser particles of slag, e.g., larger than 160  $\mu\text{m}$ , which is a major concern in milling, could be carried out efficiently using balls with intermediate size (e.g., 25.4 mm) in the initial stages, while the use of balls with varying sizes could be considered during the final stages. The results also revealed that small balls (e.g., 12.7 mm) are suitable for grinding coarse slag particles at the initial stages, while as grinding proceeds (e.g., for grinding times longer than 25 min) larger balls are needed for efficient grinding. In addition, due to the fact that, at the final grinding stages, the coarse slag particles exhibit lower breakage rate when 40 mm balls are used compared to 25.4 mm balls, it can be deduced that there is a size range  $d$  of balls (12.7 mm <  $d$  < 40 mm) which is the most suitable for slag grinding. The latter can explain that grinding media consisting of balls with varying sizes (40, 25.4, and 12.7 mm) result in a higher breakage rate (as seen in Figure 3b) during the final stages.

### 3.2. Particle Size and Specific Surface Area of Slag Products

In an effort to investigate the fineness of slag products, Table 4 presents the characteristic particle sizes of the cumulative volume distributions, i.e., the  $d_{50}$  and  $d_{90}$  for various grinding times when different ball sizes are used as grinding media.  $d_{50}$ , also known as median size, corresponds to 50% cumulative undersize, and has been successfully used to compare and evaluate different particle size distributions during grinding. In addition, the coarse part of the cumulative distributions can be represented by the characteristic particle size  $d_{90}$ . It is evident that for a given load of grinding media, the particle size of the grinding product decreases gradually with grinding time, as the values of  $d_{50}$  and  $d_{90}$  indicate. The decreasing trend of  $d_{90}$  is also an evidence that in the case of slag milling, contrary to the

findings of previous studies [63,64], no agglomeration was observed even after prolonged grinding periods (120 min). Table 4 also shows the SSA of the slag products obtained by either the application of BET or LD techniques. It is observed that the determined SSA using BET is much higher in all cases, compared to that obtained using the LD technique, as earlier studies indicate [65,66]. BET which is based on gas ( $N_2$ ) adsorption is the most widely used technique for the determination of SSA, as it takes into account several factors, including the surface roughness of particles, the presence of cracks, and the geometry of pores [67]. In this context, BET can be used to determine the actual grinding limit and the minimum particle size which could theoretically be obtained during grinding [68].

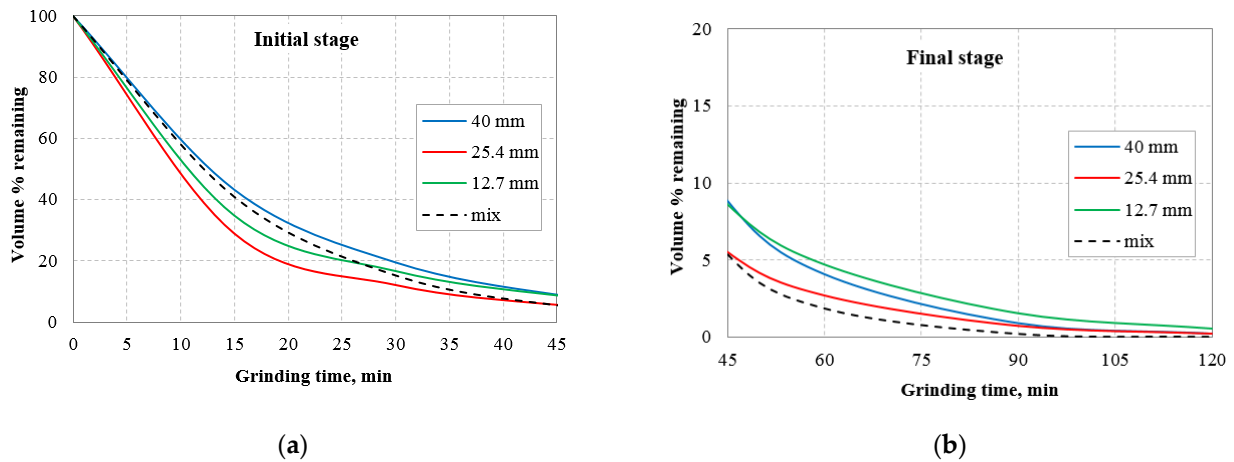


**Figure 3.** Remaining fraction (% volume) of the 163.8 μm particle size vs. grinding time at (a) the initial grinding stage, and (b) longer grinding periods; grinding media consisted of balls with various size (mix denotes a mixed load of grinding media consisting of equal mass of balls from each of the three sizes (40, 25.4, and 12.7 mm)).

**Table 4.** Characteristic particle size ( $d_{50}$  and  $d_{90}$ ) and specific surface area of slag products obtained with the use of different grinding media and grinding periods.

Ball Size (mm)	Parameter	Grinding Period (min)					
		15	30	45	60	90	120
40	$d_{90}$ (μm)	289.9	175.8	139.0	93.0	69.9	60.0
	$d_{50}$ (μm)	86.4	44.2	31.1	22.6	16.6	13.4
	BET (m <sup>2</sup> /kg)	894	1163	1378	1686	1999	2293
	LD (m <sup>2</sup> /kg)	213	301	388	489	631	750
25.4	$d_{90}$ (μm)	225.1	158.0	106.0	80.9	59.3	48.5
	$d_{50}$ (μm)	59.1	38.3	25.4	20.4	14.5	11.8
	BET (m <sup>2</sup> /kg)	1513	1852	2325	2569	3223	3547
	LD (m <sup>2</sup> /kg)	350	476	655	765	1001	1167
12.7	$d_{90}$ (μm)	254.6	196.6	127.7	80.1	53.1	40.0
	$d_{50}$ (μm)	55.3	39.2	28.4	21.7	15.2	11.2
	BET (m <sup>2</sup> /kg)	1065	1323	1485	1679	2000	2213
	LD (m <sup>2</sup> /kg)	271	341	392	511	631	764
mix *	$d_{90}$ (μm)	252.2	153.8	109.5	86.2	59.9	47.1
	$d_{50}$ (μm)	75.9	39.9	27.8	23.4	15.2	11.9
	BET (m <sup>2</sup> /kg)	930	1200	1435	1598	2160	2260
	LD (m <sup>2</sup> /kg)	221	316	416	486	682	780

\* a mixed load of grinding media consisting of equal mass of balls from each of the three sizes (40, 25.4, and 12.7 mm).

Figure 4 shows the evolution of BET size with specific energy input for the different grinding media used. BET size was determined using the specific surface area values obtained by the BET technique (Table 4) in Equation (10) for  $f/k = \pi/6$ , while the specific energy input was calculated using Equations (8) and (9). The results show that, in all cases, the slag particle size reduction during grinding can be accurately described using inverse exponential functions, as indicated by the high  $R^2$  values. It is apparent that the reduction rate is constantly decreasing and this indicates that as grinding proceeds more energy is consumed for the same size reduction. Theoretically, there is a point (grinding limit) which indicates that no further breakage of particles occurs beyond that and thus all the amount of excessive energy consumed is considered as loss. By comparing the plots of BET size versus specific energy input (Figure 4), it appears that the use of 25.4 mm balls results in much finer products. In addition, the reduction rate of BET sizes is lower when 12.7 mm balls are used, indicating that a coarser minimum particle size is obtained compared to the other grinding media used.

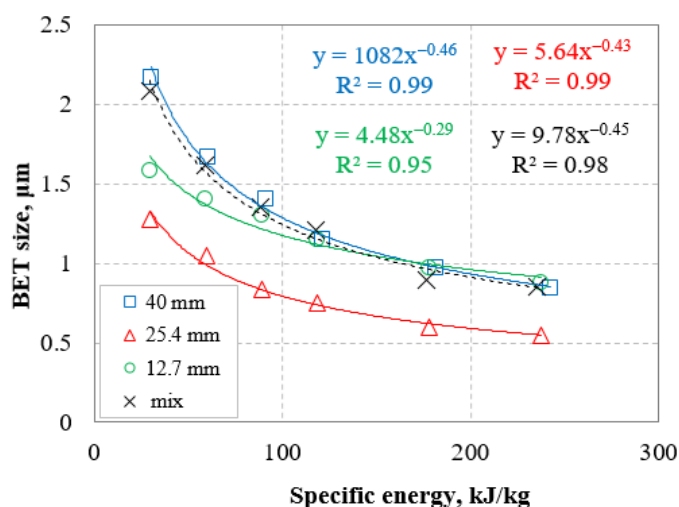


Figure 4. Evolution of Brunauer–Emmett–Teller (BET) size with specific energy when grinding media consisted of balls with various size (mix denotes a mixed load of grinding media consisting of equal mass of balls from each of the three sizes (40, 25.4, and 12.7 mm)).

The slag fineness after grinding was assessed using the following formula (Equation (11)) proposed by Tanaka [69,70],

$$\Delta S_w = \Delta S_{w\infty} \cdot [1 - \exp(-k \cdot \varepsilon)] \tag{11}$$

where  $\Delta S_w$  is the total SSA of the products for specific energy input  $\varepsilon$ ,  $\Delta S_{w\infty}$  is the SSA (maximum) at the grinding limit ( $\varepsilon = \infty$ ), and  $k$  is a constant (grinding coefficient).

Using the Excel’s Solver tool, the optimum  $\Delta S_{w\infty}$  and  $k$  values can be estimated, while the surface area production rate (SAPR) can be calculated from the derivative of Equation (11), according to Equation (12),

$$\Delta S_w' = k \cdot \Delta S_{w\infty} \cdot \exp(-k \cdot \varepsilon) \tag{12}$$

In this study, Equation (11) was applied to the experimental data, i.e., the SSA values derived from the BET technique (Table 4), by considering that the grinding limit was reached when the SAPR is equal to  $0.10 \text{ m}^2/\text{kJ}$ .

Figure 5a,b show the specific surface area (SSA) versus the specific energy for the slag grinding products when various ball sizes were used. More specifically, Figure 5a indicates that at the initial grinding stage (0–45 min) the SSA increases almost linearly with the increase of specific energy input. However, the SAPR, i.e., slope at each point of the curves, is influenced by the size of the grinding media. Among the different grinding

media tested, the 25.4 mm balls result in products with the highest SAPR, while the lowest rate is observed when 40 mm balls are used.

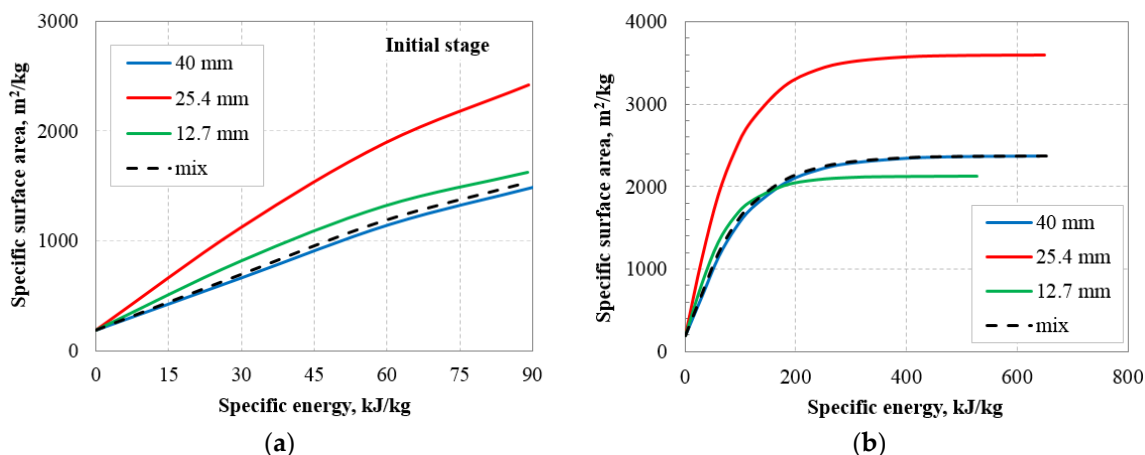


**Figure 5.** Specific surface area versus specific energy (a) at the initial grinding stages (0–45 min) and (b) at all energy levels studied; grinding media consisted of balls with various sizes (mix denotes a mixed load of grinding media consisting of equal mass of balls from each of the three sizes (40, 25.4, and 12.7 mm)).

In terms of energy efficiency, it is revealed that the 40 mm and 12.7 mm balls, as well as the mixed load of balls, cannot produce more than 1600 m<sup>2</sup>/kg SSA for a specific energy consumption of 90 kJ/kg, while the same SSA with significantly lower specific energy (~47 kJ/kg) can be produced with the use of intermediate size balls, 25.4 mm. This results in 48% decrease in energy requirements and the associated CO<sub>2</sub> emissions at the initial stages of slag grinding.

The evolution of the SSA with specific energy input for all energy levels tested (Figure 5b) reveals the difficulty in producing new surface area after prolonged grinding and that the maximum SSA (grinding limit) depends upon the grinding media used.

Overall, the results obtained at the grinding limit are shown in Table 5. It is observed that, with the use of 25.4 mm balls, a maximum SSA of 3596 m<sup>2</sup>/kg can be obtained after 240 min of grinding (or 486 kJ/kg specific energy consumption) with a BET particle size of 0.54 μm. The lowest grinding efficiency in terms of SSA production (2121 m<sup>2</sup>/kg) at the grinding limit is observed when 12.7 mm balls are used, while the use of either 40 mm balls or a mixed load of balls results in almost similar SSA values (SSA ranged from 2369 to 2376 m<sup>2</sup>/kg).

**Table 5.** Characteristic parameters at the grinding limit.

Ball Size (mm)	Specific Energy kJ/kg	Time min	SSA m <sup>2</sup> /kg	k kg/kJ	BET Size μm
40	507	258	2369	0.011	0.82
25.4	486	240	3596	0.013	0.54
12.7	357	180	2121	0.016	0.91
mix *	482	244	2376	0.012	0.81

\* A mixed load of grinding media consisting of equal mass of balls from each of the three sizes (40, 25.4, and 12.7 mm).

### 3.3. Analysis of the Attainable Region Technique

For the use of the attainable region (AR) technique, the objective function needs to be defined. In light of this, the particle size distribution of the grinding products was classified into three size classes, i.e., the coarse (class 1), the intermediate (class 2), and the fine (class 3), and the objective was to maximize the fraction of the desired size class. In

this study, the desired size class was the intermediate fraction,  $-163.8 +26 \mu\text{m}$ , and was selected by taking into account that the next most probable step of the process will be either flotation or leaching [5,71,72]. As the slag feed size investigated is smaller than  $850 \mu\text{m}$ , the coarse and fine size classes will be represented by the fractions  $(-850 +163.8 \mu\text{m})$  and  $(-26 \mu\text{m})$ , respectively.

The grinding behavior of class 1 ( $-850 +163.8 \mu\text{m}$ ) has already been discussed in previous sections. As seen in Figures 1 and 3a,b the breakage rate of this size class follows non-first-order breakage kinetics after prolonged grinding periods and its grinding rate is time-dependent. However, as seen in Figure 6, which shows the remaining volume fraction of class 1 versus grinding time at the initial grinding stages (0–45 min), for the different grinding media tested, its breakage rate obeys first-order kinetics. As a result, for the grinding period 0–45 min, the breakage rate  $S_1$  of size class 1 can be determined with the use of Equation (3).

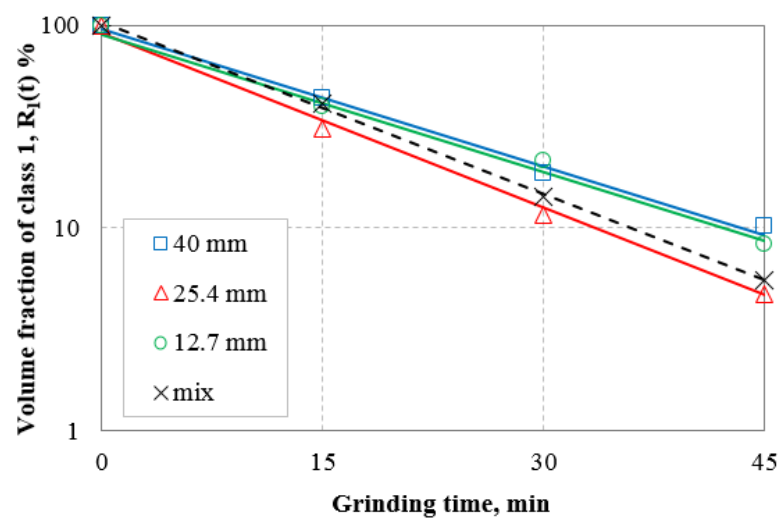


**Figure 6.** First order plots for size class 1 ( $-850 +163.8 \mu\text{m}$ ) at the initial grinding stages (0–45 min); grinding media consisted of balls with various sizes (mix denotes a mixed load of grinding media consisting of equal mass of balls from each of the three sizes (40, 25.4, and 12.7 mm)).

Table 6 shows, for the different ball sizes tested, the values of the breakage rate  $S_1$  as well as the adjusted correlation coefficient (Adj.  $R^2$ ) obtained when Equation (3) was fitted to the experimental data. It is observed that  $S_1$  increases with increasing ball size from 12.7 to 25.4 mm, while it decreases when larger balls (40 mm) are used. Therefore, there is an optimum ball size, in our case 25.4 mm, for which the breakage rate of size class 1 obtains its maximum value,  $0.066 \text{ min}^{-1}$ . Furthermore, this table also reveals that the use of a mixed load of grinding media consisting of balls with varying size (40, 25.4, and 12.7 mm) results in an equally high breakage rate ( $0.065 \text{ min}^{-1}$ ) for size class 1.

**Table 6.** The parameter values of Equations (3) and (5) for different ball sizes.

Ball Size (mm)	Equation (3)		Equation (5)		
	$S_1 \text{ (min}^{-1}\text{)}$	Adj. $R^2$	$S_2 \text{ (min}^{-1}\text{)}$	$b_{21}$	Adj. $R^2$
40	0.055	0.990	0.013	0.796	0.999
25.4	0.066	0.992	0.016	0.861	0.993
12.7	0.052	0.988	0.009	0.695	0.997
mix *	0.065	0.998	0.011	0.785	1.000

\* A mixed load of grinding media consisting of equal mass of balls from each of the three sizes (40, 25.4, and 12.7 mm).

The volume fraction of the desired size class 2 ( $-163.8 + 26 \mu\text{m}$ ) as a function of grinding time, when balls with various sizes were used, as presented in Figure 7. It is shown that in all cases, the volume fraction of class 2 increases with increasing grinding time up to a certain point, which is called the turning point, and then decreases. This implies that there is an optimal grinding time (or specific energy input) at which the maximum volume fraction of class 2 is obtained, and this time is dependent on the ball size used. This figure also shows that the same volume fraction of class 2 can be obtained with the use of different ball sizes, but at different grinding times. For example, if the desired volume fraction is 40%, it is shown that depending on the size of the grinding media, grinding times in the range of 5.3 to 9.22 min are required. In light of this, an effective way to improve slag grinding efficiency is to use 25.4 mm balls or a mixed load of balls of the same mass; 40% energy savings can be achieved compared to 12.7 mm balls. The values of the parameters  $S_2$  and  $b_{21}$  as well as the  $R^2$  (adj.) when Equation (5) was fitted to the experimental data are presented in Table 6. It is seen that the  $R^2$  (adj.) values are higher than 0.993 which indicate that Equation (5) is suitable for describing the variation of volume fraction of size class 2 with grinding time. In addition, it is observed that  $S_2$  obtains the highest value when balls with diameter 25.4 mm are used, which is not favorable for the accumulation of the desired class 2 in the products. On the other hand, the highest value of parameter  $b_{21}$  (0.861) is obtained when balls with diameter 25.4 mm are used; this indicates that a bigger mass of broken class 1 particles is present in size class 2 products. Furthermore, the results of Table 6 reveal that  $b_{21}$  obtains high values when 40 mm balls or balls with various sizes are used, 0.796 and 0.785, respectively.

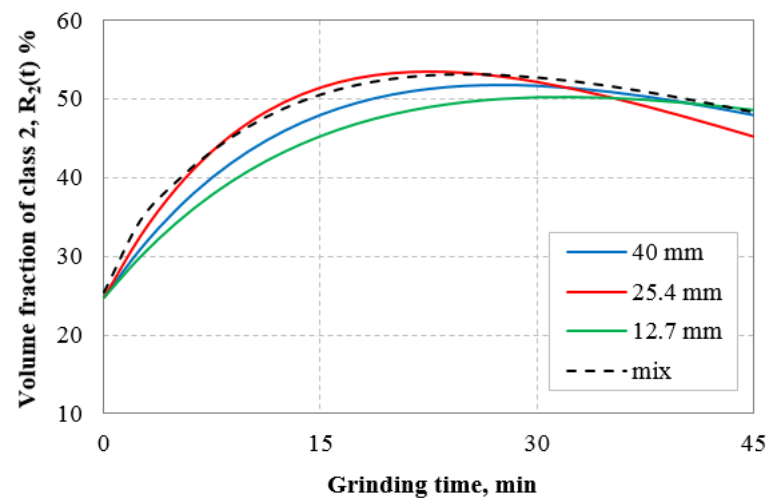


**Figure 7.** Model curves of the remaining fraction (% volume) of size class 2 vs. grinding time at the initial grinding stage (grinding time range 0–45 min), when grinding media consisted of balls with various sizes (mix denotes a mixed load of grinding media consisting of equal mass of balls from each of the three sizes (40, 25.4, and 12.7 mm)).

Table 7 presents the volume fraction of class 2, the grinding time and the specific energy consumption at the turning point when balls with various sizes are used. The use of 25.4 mm balls results in the biggest remaining volume fraction in class 2 (53.5%) after 22.5 min of grinding (or 44.6 kJ/kg specific energy consumption), while the lowest fraction of 50.3% is obtained with the use of 12.7 mm balls after 32.5 min of grinding (or 64.3 kJ/kg specific energy consumption). It is also seen that the use of a mixed load of grinding media provides similar results with those obtained with the use of 25.4 mm balls, in terms of the volume fraction of class 2 at the turning point and specific energy consumption (a volume fraction of 53.3% is obtained with an energy consumption of 49 kJ/kg). Therefore, from an energy-savings point of view, the use of either 25.4 mm balls or mixed load of balls results

in 31% and 24% lower energy requirements, respectively, compared to the use of balls with small size (12.7 mm), which indicates an equal decrease in CO<sub>2</sub> emissions.

**Table 7.** Volume fraction of class 2, grinding time and specific energy consumption at the turning point when different ball sizes were used.

Ball Size mm	Volume Fraction %	Grinding Time min	Specific Energy kJ/kg
40	51.7	27.5	55.6
25.4	53.5	22.5	44.6
12.7	50.3	32.5	64.3
mix *	53.3	25.0	49.0

\* A mixed load of grinding media consisting of equal mass of balls from each of the three sizes (40, 25.4, and 12.7 mm).

Figure 8 shows the AR plots of the volume fraction of slag in the desired size class 2 versus the volume fraction in size class 1, when different grinding media were used. Point A represents the fresh feed which is not yet ground (0 min), while the brown dashed line has a slope of 45° with the horizontal axis. At point A, the feed consists of 68.2% class 1 and 24.8% class 2, while the fraction of size class 3, calculated by the volume balance, is the remaining 7%. As grinding proceeds, the fraction of class 1 is reduced to produce size class 2 and size class 3. In this context, the volume fraction of class 2 increases until the turning point, and after that begins to decrease, indicating that further grinding would cause energy and time losses. It is reminded that, for the different grinding media used, the volume fraction of the size class of interest (class 2) at the turning point, as well as the optimum grinding time (or specific energy consumption) that maximizes the volume in this size class is presented in Table 7.

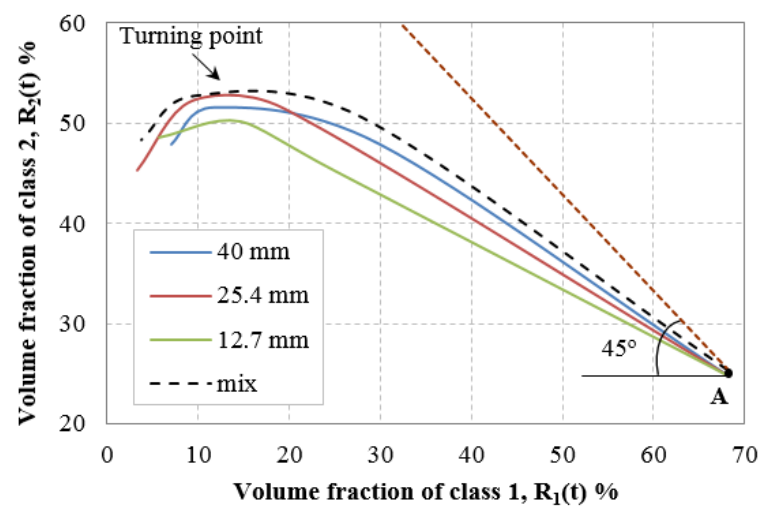


**Figure 8.** Volume fraction of size class 2 vs. volume fraction of class 1, when various ball sizes were used, including a mixed load of grinding media consisting of equal mass of balls from each of the three sizes (40, 25.4, and 12.7 mm).

In addition, it is observed from Figure 8 that during grinding the volume fraction of class 2 produced, and consequently the fraction of the undesired class 3, depend on the grinding media used. If the grinding process follows the brown dashed line, then class 1 is completely broken into class 2 and theoretically there is no production of class 3. As a result, the curves closer to the dashed line which correspond to the different grinding media used, indicate that more class 1 material is broken into class 2, rather than the undesired class 3. Thus, for a given volume fraction of class 1 more fraction of class 2 is obtained with increased ball size. In addition, the results show that when a mixed load

of grinding media is used, the production of size class 2 is promoted, and the volume of material reporting to the fine size class is reduced. For a given grinding media load, large balls impart higher impact energy and are more efficient for grinding coarse particles. A decrease in the grinding media size results in an increase in the number of balls and thus the grinding of fine particles is promoted. The use of balls with varying sizes, which is a common industrial practice in grinding circuits, may be beneficial for the production of a desired size fraction even after prolonged grinding periods, as also observed in this study.

#### 4. Conclusions

In this study grinding of ferronickel slag was investigated in a laboratory ball mill, to determine the effect of grinding media size on milling efficiency using kinetics and attainable region approaches.

Concerning slag milling kinetics, it is deduced that the remaining fraction of each representative size decreases with increasing grinding time when various grinding media are used, while the reduction rate depends on the ball size. Grinding follows non-first-order kinetics, while the grinding rate of each size fraction is time-dependent. Based on the grinding rate constant ( $K$ ) values versus particle size, it is seen that the 25.4 mm balls result in a higher breakage rate, while the rate decreases when a mixed load of grinding media is used. For the coarse particle size studied, i.e., 163.8  $\mu\text{m}$ , it was found that, the 25.4 mm balls result in the highest reduction rate during the initial stages of grinding (0–25 min), while toward the end of the initial stage (25–45 min), and at later stages (45–120 min), grinding is more efficient when a mixed load of balls with varying sizes is used.

Based on the BET technique, it was found that the use of 25.4 mm balls result in much finer product sizes and therefore, the grinding limit is reached at a finer particle size compared to the other types of grinding media used. When Tanaka's formula applied to the experimental data, it is seen that the surface area production rate at the initial stages is higher with the use of 25.4 mm balls, while a much lower rate is observed when 12.7 mm, 40 mm, or a mixed load of balls with varying size is used. This indicates that, in terms of SSA production, the energy consumption can be reduced by 48% when 25.4 mm balls are used. In addition, a maximum SSA of 3596  $\text{m}^2/\text{kg}$  with a BET particle size of 0.54  $\mu\text{m}$  at the grinding limit can be achieved with the use of 25.4 mm balls, and the use of 40 mm balls or mixed load of balls with varying size result in almost similar values (2369 and 2396  $\text{m}^2/\text{kg}$ , respectively). A much lower SSA of 2121  $\text{m}^2/\text{kg}$  is produced with the use of smaller balls (12.7 mm).

With the aim to maximize the fraction of the desired size class (class 2) which is optimum for any subsequent separation, the results of the attainable region (AR) approach showed that there is an optimum ball size (25.4 mm) for which the breakage rate of coarse size (class 1) is maximized, while the use of a mixed load of balls could also result in a similar high breakage rate of this size class. In addition, it is seen that the fraction of class 2 increases with grinding time (or specific energy input) up to a certain point (called turning point), and then decreases for longer grinding periods. Among the different ball sizes tested, the use of 25.4 mm balls or a mixed load of balls results in the largest remaining volume fraction in class 2, i.e., 53.5 and 53.3%, respectively. However, in the case of 12.7 mm balls, a maximum fraction of 50.3% of class 2 is obtained with higher specific energy consumption. In this context, the use of either 25.4 mm balls or a mixed load of balls results in 31 and 24% decrease in energy requirements, respectively, compared to 12.7 mm balls, and therefore the energy efficiency increases. Finally, from the AR plots it is seen that for a given fraction of class 1 a bigger fraction of class 2 is obtained when balls with bigger sizes are used, while the mixed load of balls with varying sizes promotes the production of this size class, and reduces the material of the fine size class (class 3).

**Author Contributions:** Conceptualization, E.P.; methodology, E.P.; writing—original draft preparation, E.P.; data analysis E.P., K.K.; writing—review and editing, K.K. All authors have read and agreed to the published version of the manuscript.

**Funding:** This research received no external funding.

**Data Availability Statement:** The data presented in this study are available on request from the corresponding author.

**Acknowledgments:** The authors wish to thank the three anonymous reviewers and the academic editor for their constructive comments, which improved the quality of the paper.

**Conflicts of Interest:** The authors declare no conflict of interest.

## References

1. Sibanda, V.; Sipunga, E.; Danha, G.; Mamvura, T.A. Enhancing the flotation recovery of copper minerals in smelter slags from Namibia prior to disposal. *Heliyon* **2020**, *6*, e03135. [[CrossRef](#)]
2. Sun, W.; Li, X.; Liu, R.; Zhai, Q.; Li, J. Recovery of Valuable Metals from Nickel Smelting Slag Based on Reduction and Sulfurization Modification. *Minerals* **2021**, *11*, 1022. [[CrossRef](#)]
3. Gabasiane, T.S.; Danha, G.; Mamvura, T.A.; Mashifana, T.; Dzinomwa, G. Characterization of copper slag for beneficiation of iron and copper. *Heliyon* **2021**, *7*, e06757. [[CrossRef](#)]
4. Piatak, N.M.; Parsons, M.B.; Seal, R.R., II. Characteristics and environmental aspects of slag: A review. *Appl. Geochem.* **2015**, *57*, 236–266. [[CrossRef](#)]
5. Roy, S.; Datta, A.; Rehani, S. Flotation of copper sulphide from copper smelter slag using multiple collectors and their mixtures. *Int. J. Miner. Process.* **2015**, *143*, 43–49. [[CrossRef](#)]
6. Guo, Z.; Zhu, D.; Pan, J.; Zhang, F. Innovative methodology for comprehensive and harmless utilization of waste copper slag via selective reduction-magnetic separation process. *J. Clean. Prod.* **2018**, *187*, 910–922. [[CrossRef](#)]
7. Gao, F.; Huang, Z.; Li, H.; Li, X.; Wang, K.; Hamza, M.F.; Wei, Y.; Fujita, T. Recovery of magnesium from ferronickel slag to prepare hydrated magnesium sulfate by hydrometallurgy method. *J. Clean. Prod.* **2021**, *303*, 127049. [[CrossRef](#)]
8. Komnitsas, K.; Zaharaki, D.; Perdikatsis, V. Effect of synthesis parameters on the compressive strength of low-calcium ferronickel slag inorganic polymers. *J. Hazard. Mater.* **2009**, *161*, 760–768. [[CrossRef](#)]
9. Mehta, A.; Siddique, R. Sustainable geopolymer concrete using ground granulated blast furnace slag and rice husk ash: Strength and permeability properties. *J. Clean. Prod.* **2018**, *205*, 49–57. [[CrossRef](#)]
10. Bartzas, G.; Komnitsas, K. Life cycle assessment of ferronickel production in Greece. *Resour. Conserv. Recycl.* **2015**, *105*, 113–122. [[CrossRef](#)]
11. Komnitsas, K.; Bartzas, G.; Karmali, V.; Petrakis, E.; Kurylak, W.; Pietek, G.; Kanasiewicz, J. Assessment of alkali activation potential of a Polish ferronickel slag. *Sustainability* **2019**, *11*, 1863. [[CrossRef](#)]
12. Gao, D.; Wang, F.-P.; Wang, Y.-T.; Zeng, Y.-N. Sustainable Utilization of Steel Slag from Traditional Industry and Agriculture to Catalysis. *Sustainability* **2020**, *12*, 9295. [[CrossRef](#)]
13. Holmberg, K.; Kivikytö-Reponen, P.; Härkisaari, P.; Valtonen, K.; Erdemir, A. Global energy consumption due to friction and wear in the mining industry. *Tribol. Int.* **2017**, *115*, 116–139. [[CrossRef](#)]
14. Jeswiet, J.; Szeker, A. Energy Consumption in Mining Comminution. *Procedia CIRP* **2016**, *48*, 140–145. [[CrossRef](#)]
15. Petrakis, E.; Komnitsas, K. Development of a Non-linear Framework for the Prediction of the Particle Size Distribution of the Grinding Products. *Mining Metall. Explor.* **2021**, *38*, 1253–1266. [[CrossRef](#)]
16. Komnitsas, K.; Yurramendi, L.; Bartzas, G.; Karmali, V.; Petrakis, E. Factors affecting co-valorization of fayalitic and ferronickel slags for the production of alkali activated materials. *Sci. Total Environ.* **2020**, *721*, 137753. [[CrossRef](#)]
17. Branca, T.A.; Colla, V.; Algermissen, D.; Granbom, H.; Martini, U.; Morillon, A.; Pietruck, R.; Rosendahl, S. Reuse and Recycling of By-Products in the Steel Sector: Recent Achievements Paving the Way to Circular Economy and Industrial Symbiosis in Europe. *Metals* **2020**, *10*, 345. [[CrossRef](#)]
18. Stamboliadis, E. A contribution to the relationship of energy and particle size in the comminution of brittle particulate materials. *Miner. Eng.* **2002**, *15*, 707–713. [[CrossRef](#)]
19. Austin, L.G.; Klimpel, R.R.; Luckie, P.T. *Process Engineering of Size Reduction: Ball Milling*; SME–AIME: New York, NY, USA, 1984.
20. Wills, B.A.; Finch, J. *Will's Mineral Processing Technology. An Introduction to the Practical Aspects of Ore Treatment and Mineral Recovery*, 8th ed.; Butterworth-Heinemann: Oxford, UK, 2016.
21. Faria, P.M.C.; Rajamani, R.K.; Tavares, L.M. Optimization of Solids Concentration in Iron Ore Ball Milling through Modeling and Simulation. *Minerals* **2019**, *9*, 366. [[CrossRef](#)]
22. Deniz, V.; Onur, T. Investigation of the breakage kinetics of pumice samples as dependent on powder filling in a ball mill. *Int. J. Miner. Process.* **2002**, *67*, 71–78. [[CrossRef](#)]
23. Chimwani, N.; Glasser, D.; Hildebrandt, D.; Metzger, M.J.; Mulenga, F.K. Determination of the milling parameters of a platinum group minerals ore to optimize product size distribution for flotation purposes. *Miner. Eng.* **2013**, *43–44*, 67–78. [[CrossRef](#)]
24. Simba, K.P.; Moys, M.H. Effects of mixtures of grinding media of different shapes on milling kinetics. *Miner. Eng.* **2014**, *61*, 40–46. [[CrossRef](#)]
25. Petrakis, E.; Stamboliadis, E.; Komnitsas, K. Identification of optimal mill operating parameters during grinding of quartz with the use of population balance modelling. *KONA Powder Part. J.* **2017**, *34*, 213–223. [[CrossRef](#)]

26. Celik, M.S. Acceleration of breakage rates of anthracite during grinding in a ball mill. *Powder Technol.* **1988**, *54*, 227–233. [[CrossRef](#)]
27. Rajamani, R.K.; Guo, D. Acceleration and deceleration of breakage rates in wet ball mills. *Int. J. Miner. Process.* **1992**, *34*, 103–118. [[CrossRef](#)]
28. Bilgili, E.; Scarlett, B. Population balance modeling of nonlinear effects in milling processes. *Powder Technol.* **2005**, *153*, 59–71. [[CrossRef](#)]
29. Deniz, V. The effect of mill speed on kinetic breakage parameters of clinker and limestone. *Cem. Concr. Res.* **2004**, *34*, 1365–1371. [[CrossRef](#)]
30. Katubilwa, F.M.; Moys, M.H. Effect of ball size distribution on milling rate. *Miner. Eng.* **2009**, *22*, 1283–1288. [[CrossRef](#)]
31. Deniz, V. The effects of ball filling and ball diameter on kinetic breakage parameters of barite powder. *Adv. Powder Technol.* **2012**, *23*, 640–646. [[CrossRef](#)]
32. Shin, H.; Lee, S.; Suk Jung, H.; Kim, J.-B. Effect of ball size and powder loading on the milling efficiency of a laboratory-scale wet ball mill. *Ceram. Int.* **2013**, *39*, 8963–8968. [[CrossRef](#)]
33. Olejnik, T.P. Selected mineral materials grinding rate and its effect on product granulometric composition. *Physicochem. Probl. Miner. Proc.* **2013**, *49*, 407–418.
34. Mulenga, F.K.; Moys, M.H. Effects of slurry filling and mill speed on the net power draw of a tumbling ball mill. *Miner. Eng.* **2014**, *56*, 45–56. [[CrossRef](#)]
35. Umucu, Y.; Altınigne, M.Y.; Deniz, V. The effects of ball types on breakage parameters of barite. *J. Pol. Min. Eng. Soc.* **2014**, *15*, 113–117.
36. Harris, C.C. The Alyavdin-Weibull Plot of Grinding Data and the Order of Kinetics. *Powder Technol.* **1973**, *7*, 123–127. [[CrossRef](#)]
37. Guo, W.; Han, Y.; Gao, P.; Li, Y.; Tang, Z. Effect of feed size on residence time and energy consumption in a stirred mill: An attainable region method. *Powder Technol.* **2021**, *379*, 485–493. [[CrossRef](#)]
38. Horn, F. Attainable and non-attainable regions in chemical reaction technique. In Proceedings of the Third European Symposium on Chemical Reaction Engineering, Amsterdam, The Netherlands, 15–17 September 1964; Pergamon Press Ltd.: London, UK, 1964.
39. Khumalo, N.; Glasser, D.; Hildebrandt, D.; Hausberger, B.; Kauchali, S. The application of the attainable region analysis to comminution. *Chem. Eng. Sci.* **2006**, *61*, 5969–5980. [[CrossRef](#)]
40. Guo, W.; Gao, P.; Tang, Z.; Han, Y.; Meng, X. Effect of grinding media properties and stirrer tip speed on the grinding efficiency of a stirred mill. *Powder Technol.* **2021**, *382*, 556–565. [[CrossRef](#)]
41. Petrakis, E.; Komnitsas, K. Modeling of bauxite ore wet milling for the improvement of process and energy efficiency. *Circ. Econ. Sustain.* **2021**, 1–15. [[CrossRef](#)]
42. Tsave, P.K.; Kostoglou, M.; Karapantsios, T.D.; Lazaridis, N.K. A Hybrid Device for Enhancing Flotation of Fine Particles by Combining Micro-Bubbles with Conventional Bubbles. *Minerals* **2021**, *11*, 561. [[CrossRef](#)]
43. Egan, J.; Bazin, C.; Hodouin, D. Effect of particle size and grinding time on gold dissolution in cyanide solution. *Minerals* **2016**, *6*, 68. [[CrossRef](#)]
44. Chimwani, N.; Mohale, T.M.; Bwalya, M.M. Tailoring ball mill feed size distribution for the production of a size-graded product. *Miner. Eng.* **2019**, *141*, 105891. [[CrossRef](#)]
45. Metzger, M.J.; Glasser, D.; Hausberger, B.; Hildebrandt, D.; Glasser, B.J. Use of the attainable region analysis to optimize particle breakage in a ball mill. *Chem. Eng. Sci.* **2009**, *64*, 3766–3777. [[CrossRef](#)]
46. Katubilwa, F.M.; Moys, M.H.; Glasser, D.; Hildebrandt, D. An attainable region analysis of the effect of ball size on milling. *Powder Technol.* **2011**, *210*, 36–46. [[CrossRef](#)]
47. Mulenga, F.K.; Chimwani, N. Introduction to the use of the attainable region method in determining the optimal residence time of a ball mill. *Int. J. Miner. Process.* **2013**, *125*, 39–50. [[CrossRef](#)]
48. Chimwani, N.; Mulenga, F.K.; Hildebrandt, D.; Glasser, D.; Bwalya, M.M. Use of the attainable region method to simulate a full-scale ball mill with a realistic transport model. *Miner. Eng.* **2015**, *73*, 116–123. [[CrossRef](#)]
49. Kierczak, J.; Neel, C.; Puziewicz, J.; Bril, H. The Mineralogy and weathering of slag produced by the smelting of lateritic Ni ores, Szklary, Southwestern Poland. *Can. Miner.* **2009**, *47*, 557–572. [[CrossRef](#)]
50. Petrakis, E.; Karmali, V.; Bartzas, G.; Komnitsas, K. Grinding kinetics of slag and effect of final particle size on the compressive strength of alkali activated materials. *Minerals* **2019**, *9*, 714. [[CrossRef](#)]
51. Bond, F.C. Crushing and grinding calculations. *Br. Chem. Eng.* **1961**, *6*, 378–385; 543–548.
52. Gupta, A.; Yan, D.S. *Mineral Processing Design and Operations: An Introduction*, 1st ed.; Elsevier: Amsterdam, The Netherlands, 2006.
53. Li, M.; Wilkinson, D.; Patchigolla, K. Comparison of particle size distributions measured using different techniques. *Part. Sci. Technol.* **2005**, *23*, 265–284. [[CrossRef](#)]
54. Ferraris, C.; Garboczi, E.J. Identifying improved standardized tests for measuring cement particle size and surface area. *Transport. Res. Rec.* **2013**, *2342*, 10–16. [[CrossRef](#)]
55. Kuila, U.; Prasad, M. Specific surface area and pore-size distribution in clays and shales. *Geophys. Prospect.* **2012**, *61*, 341–362. [[CrossRef](#)]
56. Kotake, N.; Daibo, K.; Yamamoto, T.; Kanda, Y. Experimental investigation on a grinding rate constant of solid materials by a ball mill—Effect of ball diameter and feed size. *Powder Technol.* **2004**, *143–144*, 196–203. [[CrossRef](#)]
57. Erdem, A.S.; Ergun, S.L. The effect of ball size on breakage rate parameter in a pilot scale ball mill. *Miner. Eng.* **2009**, *22*, 660–664. [[CrossRef](#)]

58. Magdalinovic, N.; Trumic, M.; Trumic, M.; Andric, L. The optimal ball diameter in a mill. *Physicochem. Probl. Miner. Process.* **2012**, *48*, 329–339.
59. Cayirli, S. Influences of operating parameters on dry ball mill performance. *Physicochem. Probl. Miner. Process.* **2018**, *54*, 751–762.
60. Petrakis, E.; Karmali, V.; Komnitsas, K. Factors affecting nickel upgrade during selective grinding of low-grade limonitic laterites. *Miner. Process. Ext. Metall.* **2021**, *130*, 192–201. [[CrossRef](#)]
61. Petrakis, E.; Komnitsas, K. Effect of Energy Input in a Ball Mill on Dimensional Properties of Grinding Products. *Mining Metall. Explor.* **2019**, *36*, 803–816. [[CrossRef](#)]
62. Cho, H.; Kwon, J.; Kim, K.; Mun, M. Optimum choice of the make-up ball sizes for maximum throughput in tumbling ball mills. *Powder Technol.* **2013**, *246*, 625–634. [[CrossRef](#)]
63. Zhao, J.; Wang, D.; Yan, P.; Li, W. Comparison of grinding characteristics of converter steel slag with and without pretreatment and grinding aids. *Appl. Sci.* **2016**, *6*, 237. [[CrossRef](#)]
64. Bouaziz, A.; Hamzaoui, R.; Guessasma, S.; Lakhal, R.; Achoura, D.; Leklou, N. Efficiency of high energy over conventional milling of granulated blast furnace slag powder to improve mechanical performance of slag cement paste. *Powder Technol.* **2017**, *308*, 37–46. [[CrossRef](#)]
65. Gómez-Tena, M.P.; Gilabert, J.; Toledo, J.; Zumaquero, E.; Machí, C. Relationship between the specific surface area parameters determined using different analytical techniques. In Proceedings of the XIII World Congress on Ceramic Tile Quality, Castellon, Spain, 17–18 February 2014; pp. 1–10.
66. Alderete, N.M.; Villagran Zaccardi, Y.; Coelho Dos Santos, G.S.; De Belie, N. Particle Size Distribution and Specific Surface Area of SCM's Compared Through Experimental Techniques. In *Proceeding of the Int. RILEM Conference on Materials, Systems and Structures in Civil Engineering—Segment on Concrete with Supplementary Cementitious Materials, Lungby, Denmark, 22–24 August 2016*; Jensen, O.M., Kovler, K., De Belie, N., Eds.; RILEM: Paris, France, 2016; pp. 61–70.
67. Cepuritis, R.; Garboczi, E.J.; Ferraris, C.F.; Jacobsen, S.; Sørensen, B.E. Measurement of particle size distribution and specific surface area for crushed concrete aggregate fines. *Adv. Powder Technol.* **2017**, *28*, 706–720. [[CrossRef](#)]
68. Knieke, C.; Sommer, M.; Peukert, W. Identifying the apparent and true grinding limit. *Powder Technol.* **2009**, *195*, 25–30. [[CrossRef](#)]
69. Tanaka, T. A new concept applying a final fineness value to grinding mechanism-grinding tests with frictional and impulsive force. *Kagaku Kogaku* **1954**, *18*, 160–171. [[CrossRef](#)]
70. Choi, H.; Lee, W.; Kim, S. Effect of grinding aids on the kinetics of fine grinding energy consumed of calcite powders by a stirred ball mill. *Adv. Powder Technol.* **2009**, *20*, 350–354. [[CrossRef](#)]
71. Gu, F.; Zhang, Y.; Peng, Z.; Su, Z.; Tang, H.; Tian, W.; Liang, G.; Lee, J.; Rao, M.; Li, G.; et al. Selective recovery of chromium from ferronickel slag via alkaline roasting followed by water leaching. *J. Hazard. Mater.* **2019**, *374*, 83–91. [[CrossRef](#)]
72. Cao, R.; Jia, Z.; Zhang, Z.; Zhang, Y.; Banthia, N. Leaching kinetics and reactivity evaluation of ferronickel slag in alkaline conditions. *Cem. Concr. Res.* **2020**, *137*, 106202. [[CrossRef](#)]